

Simultaneous generation and Brillouin amplification of a dark hollow beam with a liquid-core optical fiber

Wei Gao,* Xiaobo Hu, Di Sun, and Jianyi Li

Department of optics information science and technology, Harbin University of Science and Technology, Harbin 150001, China

**wei_g@163.com*

Abstract: We propose and demonstrate a new method to generate a dark hollow beam (DHB) and amplify it simultaneously by a liquid-core optical fiber (LCOF) filled with CS₂. A DHB with an adjustable dark spot size (DSS) is simply obtained by changing the incident angle of the laser beam. Based on non-collinear Brillouin amplification, a weak DHB can be amplified with high gain. The amplification factor of 10⁶ is achieved for a DHB of 4pJ. This DHB should have promising applications in many fields due to its compact structure, low cost, wide adjustment range of the DSS, and wide operating wavelength.

©2012 Optical Society of America

OCIS codes: (190.0190) Nonlinear optics; (190.2640) Stimulated scattering, modulation, etc.; (290.5830) Scattering, Brillouin; (080.4865) Optical vortices.

References and links

1. M. Y. Zhang, S. Q. Li, Y. Y. Yao, B. Fu, and L. Zhang, "A dark hollow beam from a selectively liquid-filled photonic crystal fibre," *Chin. Phys. B* **19**(4), 47103–47108 (2010).
2. Q. G. Sun, K. Y. Zhou, G. Y. Fang, G. Q. Zhang, Z. J. Liu, and S. T. Liu, "Hollow sinh-Gaussian beams and their paraxial properties," *Opt. Express* **20**(9), 9682–9691 (2012).
3. Z. Y. Chen and D. M. Zhao, "4Pi focusing of spatially modulated radially polarized vortex beams," *Opt. Lett.* **37**(8), 1286–1288 (2012).
4. R. Chakraborty and A. Ghosh, "Generation of an elliptic hollow beam using Mathieu and Bessel functions," *J. Opt. Soc. Am. A* **23**(9), 2278–2282 (2006).
5. H. Ito, K. Sakaki, W. Jhe, and M. Ohtsu, "Atomic funnel with evanescent light," *Phys. Rev. A* **56**(1), 712–718 (1997).
6. W. L. Power, L. Allen, M. Babiker, and V. E. Lembessis, "Atomic motion in light beams possessing orbital angular momentum," *Phys. Rev. A* **52**(1), 479–488 (1995).
7. N. R. Heckenberg, R. McDuff, C. P. Smith, and A. G. White, "Generation of optical phase singularities by computer-generated holograms," *Opt. Lett.* **17**(3), 221–223 (1992).
8. J. P. Yin, H. R. Noh, K. Lee, K. H. Kim, Y. Z. Wang, and W. H. Jhe, "Generation of a dark hollow beam by a small hollow fiber," *Opt. Commun.* **138**(4-6), 287–292 (1997).
9. H. Y. Ma, H. D. Cheng, W. Z. Zhang, L. Liu, and Y. Z. Wang, "Generation of a hollow laser beam by a multimode fiber," *Chin. Opt. Lett.* **5**, 460–462 (2007).
10. X. B. Zhang, X. Zhu, X. Chen, H. Q. Li, J. G. Peng, N. L. Dai, and J. Y. Li, "A hollow beam supercontinuum generation by the supermode superposition in a GeO₂ doped triangular-core photonic crystal fiber," *Opt. Express* **20**(18), 19799–19805 (2012).
11. Y. G. Zhao, Z. P. Wang, H. H. Yu, S. D. Zhuang, H. Zhang, X. D. Xu, J. Xu, X. G. Xu, and J. Y. Wang, "Direct generation of optical vortex pulses," *Appl. Phys. Lett.* **101**(3), 031113 (2012).
12. H. C. Liang, Y. J. Huang, Y. C. Lin, T. H. Lu, Y. F. Chen, and K. F. Huang, "Picosecond optical vortex converted from multigigahertz self-mode-locked high-order Hermite-Gaussian Nd:GdVO₄ lasers," *Opt. Lett.* **34**(24), 3842–3844 (2009).
13. J. P. Yin, N. C. Liu, Y. Xia, and M. Yun, "Generation of hollow laser beams and their applications in modern optics," *Prog. Phys.* **24**, 336–380 (2004).
14. K. Yamane, Y. Toda, and R. Morita, "Ultrashort optical-vortex pulse generation in few-cycle regime," *Opt. Express* **20**(17), 18986–18993 (2012).
15. F. F. Dai, Y. H. Xu, and X. F. Chen, "Tunable and low bending loss of liquid-core fiber," *Chin. Opt. Lett.* **8**(1), 14–17 (2010).
16. W. Gao, D. Sun, Y. F. Bi, J. Y. Li, and Y. L. Wang, "Stimulated Brillouin scattering with high reflectivity and fidelity in liquid-core optical fibers," *Appl. Phys. B* **107**(2), 355–359 (2012).

17. W. Gao, Z. W. Lu, W. M. He, Y. K. Dong, and W. L. J. Hasi, "Characteristics of amplified spectrum of a weak frequency-detuned signal in a Brillouin amplifier," *Laser Part. Beams* **27**(03), 465–470 (2009).
 18. Z. W. Lu, W. Gao, W. M. He, Z. Zhang, and W. L. J. Hasi, "High amplification and low noise achieved by a double-stage non-collinear Brillouin amplifier," *Opt. Express* **17**(13), 10675–10680 (2009).
 19. W. Gao, Z. W. Lu, W. M. He, and C. Y. Zhu, "Investigation on competition between the input signal and noise in a Brillouin amplifier," *Appl. Phys. B* **105**(2), 317–321 (2011).
 20. G. P. Agrawal, *Nonlinear Fiber Optics* (Elsevier Pte Ltd., Singapore, 2009), Chap. 9.
-

1. Introduction

A ring beam with zero central intensity along the beam axis is called as a dark hollow beam (DHB), which has attracted great attention in recent years because of its wide applications in atom trapping and guiding, free space optical communication, laser processing, and life science [1–4]. Many techniques have been used to generate the DHBs, such as geometrical optical method, mode conversion, optical holography and so on [5–7]. The experimental arrangements of these methods are usually more complicated. Afterward, some simpler methods such as a small hollow fiber, multimode fiber, and photonic crystal fiber (PCF) have been presented [8–10]. However, a hollow fiber has disadvantages of low coupling efficiency and large loss due to its small core contained air [8]; the dark spot size (DSS) of the DHB produced with a multimode fiber can be changed by adjusting the angle between the laser beam and the fiber axis (i. e. incident angle). Owing to a small numerical aperture (NA, about 0.3) of multimode fibers the incident angle has a small adjusting range, which is only $\pm 2.78^\circ$, as a result, the DSS span of the DHB is confined and the DHB corresponding to a larger angle is too weak to be applied in practice [9]; special PCFs require complex process, and the production cost is higher [1, 10]. Most of the previous investigations of DHBs were focused on continuous wave operation. However, high energy DHB pulses are being paid more attention recently [10, 11], since they are urgently demanded in various fields, including material processing, trapping free electrons with high efficiency, and high-field laser physics [12–14].

Liquid-core optical fiber (LCOF) consists of flexible capillary tubing filled with liquids characterized by sufficiently high refractive indices. In contrast to the traditional crystal fiber, the LCOF has advantages of large NA, small bending loss, and wide operating wavelength range [15]. For instance, the NA of the LCOF filled with CS_2 is about 0.68, and corresponding to the half of receiving angle of about 20° . The experiments demonstrated that the stimulated Brillouin scattering (SBS) in a LCOF has low SBS threshold, high reflectivity, and high pulse-shape and phase-conjugation fidelity [16]. Brillouin amplification for a weak signal using a LCOF, to our knowledge, has not been investigated.

To solve above-mentioned problems such as low generating efficiency, small NA, large loss, and complex structure, we propose a technique to generate the DHB by a LCOF, and introduce non-collinear Brillouin amplification to improve the DHB pulse energy. By using this method, not only can the DHB's DSS be changed over a large size range but also its frequency can also be tuned by choosing mixing medium as core-liquid material.

2. Theory

2.1 Generation of a DHB

The output beams passing through a LCOF are simulated by a ray tracing method using the non-sequential analysis function module of the optical design software named Zemax. The simulating model is shown in Fig. 1. In the calculation, the following parameters are used: the incident laser beam has the wavelength of 532 nm and a Gaussian intensity profile; tracing 10^7 rays; the focal length of the lens $f = 50\text{mm}$; the distance between the lens and the front end of the LCOF $d_i = 40\text{mm}$; CS_2 is chosen as the core-liquid medium, its refractive index $n_{\text{core}} = 1.62$; the refractive index of the quartz cladding $n_{\text{clad}} = 1.465$; the incident angle $\theta = 0^\circ$ – 12° ; the distance between the output end of the LCOF and the screen $d_o = 20\text{mm}$.

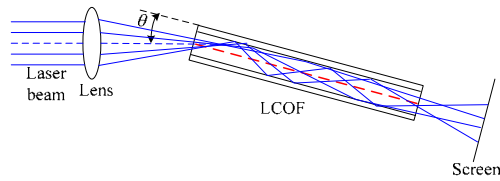


Fig. 1. Modeling schematic of generating a DHB by a LCOF.

Figure 2 depicts the dependence of the DHB's DSS on the incident angle of the laser beam. The DSS is defined as the full-width half-maximum (FWHM) of the radial intensity distribution of the DHB sunken inside (see the inset of Fig. 2). We notice that the output beam is a solid spot for the incident angle of 0° . With increasing the incident angle a dark spot appears at the center of output beam, and thus the DHB is generated. Moreover, the DSS increases with the angle. Generally speaking, there are two kinds of rays in the LCOF, which are the meridian and skew rays, respectively. For the case of $\theta = 0^\circ$, the focused incidence spot by the lens is located on the axis of the fiber, thus the laser beams travelled in the fiber are meridian rays, which form a high power or energy density at the center of the fiber core. When the incident angle increases, the focused spot will be off the axis, as a result, many skew rays are excited. As we know, those skew rays propagate along a spiral path through the fiber, leading high power density zone to the edge of the fiber core. At this time, a kind of mode with the dark core spot is selectively excited, like a doughnut beam. Moreover, the larger the angle, the greater the caustic aperture of skew rays propagation, and hence the larger DSS.

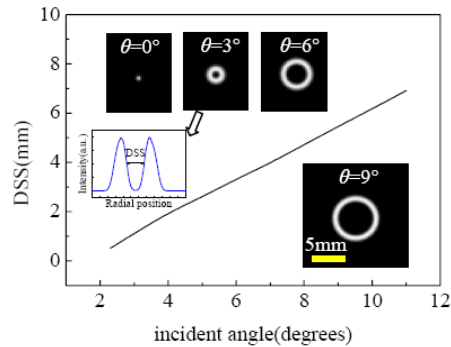


Fig. 2. DSS versus the incident angle θ of the laser beam. Inset, the beam spot images of the DHBs at the incident angles of 0° , 3° , 6° and 9° , and the radial intensity distribution of the DHB at 3° .

2.2 Basic principle of non-collinear Brillouin amplification in a LCOF

In Brillouin amplification, a signal beam and a counterpropagating pump beam interfere in a nonlinear medium and drive an acoustic wave, which in turn scatters light from the pump beam to produce an amplified signal beam. For obtaining the maximum gain, the signal beam must satisfy the following two conditions: one is frequency matching, i.e., the frequency difference between the signal and the pump beams should be equal to the Brillouin shift of nonlinear medium; two is that the polarization direction of the signal should be coincident with that of the pump. To achieve Brillouin amplification of the DHB, the signal beam (E_s) and the pump beam (E_p) are coupled into a LCOF from its opposite ends at angles of θ_s and θ_p , respectively, as shown in Fig. 3. Here θ_s and θ_p should be less than the receiving angle limited by NA. The single transversal mode signal beam striking at θ_s propagates in the LCOF, as mentioned above, the transmission output without the pump appears as the DHB. Once the pump beam is introduced, the DHB generated will be amplified at the same time.

This indicates that the spatial distribution of amplified beam mainly depends on the signal output without the pump, not input. Furthermore, the DHB frequency can be tuned by using the mixture as core material. This is because the frequency shift of the amplified signal with respect to the pump is mainly determined by the Brillouin shift of core-liquid medium [17], and the Brillouin shift of the mixture changes with the mixing ratio.

The reasons for introducing the off-axis pump beam have two aspects: on one hand, it is convenient to extract amplified DHB; on the other hand, the noise output of the LCOF amplifier can be spatially separated from the signal channel by choosing proper system parameters [18]. This off-axis input is also called as non-collinear structure.

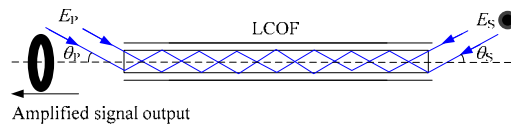


Fig. 3. Schematic diagram of non-collinear interaction of the pump and signal beams in a LCOF.

3. Experiment

The experimental setup for generating DHBs is similar to the structure of the simulating model shown in Fig. 1. A 532nm wavelength single-mode laser is used as a laser source. The laser beam is focused by a lens with focal length of 50mm. The CS₂ LCOF is fixed on the five-dimension adjuster. The incident angle of the laser beam can be changed by adjusting the LCOF. The length and core diameter of the LCOF are 50cm and 400 μ m, respectively. The output beam patterns are recorded at about 10mm away from the end of the LCOF by CCD (KOCA KA-1881) instead of the screen in Fig. 1.

Near field patterns of output beams for several incident angles are shown in Fig. 4. The output patterns evolve from a solid spot to the DHBs with different DSSs, and the DSS increases with the incident angle. In practice, the DHB output at the angle of 20° are also observed in the screen, but not be recorded by CCD because of its limited receiving area. Different from the multimode-fiber method [9], the beam patterns such as misty light spot in the ring core and double rings were not observed.

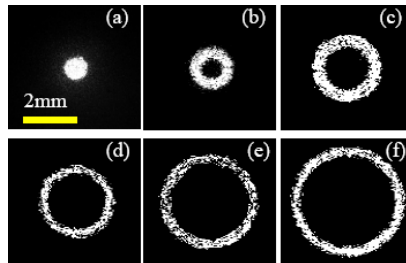


Fig. 4. Near field patterns of output beams for different incident angles. (a) 0°; (b) 3°; (c) 7°; (d) 9°; (e) 12°; (f) 14°

The experimental setup of simultaneous generation and amplification of DHBs is depicted in Fig. 5. A passively *Q*-switched ND:YAG laser produces single longitudinal quasi-Gaussian pulses with duration 10ns and linear polarization at 1Hz repetition rate. An aperture of 1.5mm is inserted into the cavity to limit the higher transversal modes. After passing through second harmonic generator and short-wave pass filter, the output light has a wavelength of 532nm. The laser beam passes through a half-wave plate ($\lambda/2$), and is split into two beams by a polarized beam splitter (PBS₁). The reflected beam is directed toward the SBS cell contained CS₂. The returning Stokes beam is used as an input signal whose energy is varied by calibrated neutral-density filters (ND). The transmitted beam from PBS₁ is used to form a pump beam. The pump energy is continuously varied by means of an attenuator, which

consisted of a rotatable half-wave plate ($\lambda/2$) and a polarized beam splitter (PBS₂). The pump and signal beams are introduced to the LCOF by lenses L₂ and L₃ ($f = 50\text{mm}$) at certain incident angles, respectively. These two beams interact in the 50cm-long and 400 μm core-diameter LCOF contained CS₂, and amplified signal beam is detected by CCD or energy meter at the output position. Different energy detectors (Ophir PE-9, PD-10 and Newport 818E-10-25-S) are used according to the values of laser energy.

According to Ref [19], the delay time that the pump pulse enters the amplifier with respect to the signal pulse has great influence on the suppression of amplified spontaneous Brillouin scattering, signal amplification factor (SAF), and signal-noise-ratio. The delay time should be controlled as the pump pulse half-width to improve the amplifier performance. In the experiment, the delay layout is designed to obtain the delay time of 5ns.

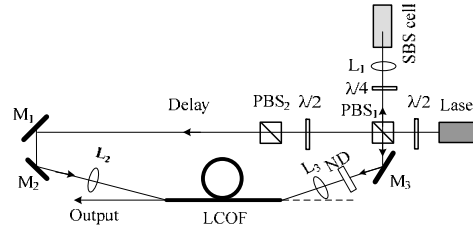


Fig. 5. Experimental setup of non-collinear Brillouin amplification in a LCOF.

To validate simultaneous generation and amplification of a DHB, output spot images of the amplifier are illustrated in Fig. 6, where Fig. 6(a) and 6(b) correspond to the output signal spots with the pump off and on for the pump and signal beams all at 0° incidence, respectively; while Fig. 6(c) and 6(d) are output spots with the pump off and on for the pump at the incident angle of 9° and the signal of 6°, respectively. We see that the spot of amplified output signal follows the unamplified output one not input signal. During the interaction of the pump with the signal beams at a certain angle, the DHB is produced and amplified. Noting from Fig. 6(d) that the pump self-SBS noise(right small spot) is separated from the amplified DHB by using non-collinear amplification structure, and is very easy to be removed with a filter homemade.

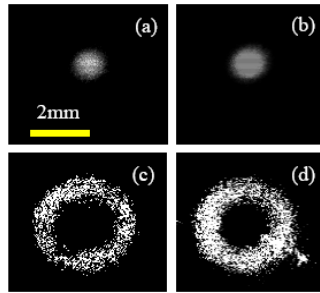


Fig. 6. Spot images of amplifier output (a), (c) with the pump off and (b), (d) with the pump on. (a), (b): the incident angles of the pump and signal are all 0°; (c), (d): the incident angles of the pump and signal are 9° and 6°, respectively.

We measure SAF of the DHB for the case of Fig. 6(c) and 6(d). SAF is defined as the ratio of the output signal energy with the pump on to the output signal energy with the pump off, thus removing effects due to Fresnel reflection, absorption, and scattering. The pump self-SBS noise is also effectively filtered. Firstly, the optimum working point E_{opt} of the LCOF amplifier is determined. Figure 7(a) shows the dependence of the SAF on the pump input energy E_{pin} . In the experiment, the signal input energy E_{sin} is set as 0.25nJ. It is seen that high SAF is obtained when E_{pin} is above the SBS threshold value E_{SBsth} , so E_{opt} are chosen at nearly saturated amplification [19]. At this time, although SBS takes place, SBS reflectivity is

usually below 30%, and there is still enough pump energy to be transferred to the signal. The relative stability of the amplified DHB energy is approximately 5%, which can be further improved by producing the Stokes-shifted signal with microwave generator and intensity modulator or a tunable laser. This is because the inherent instability of the returning Stokes beam back from the SBS cell has direct effect on the amplified output. Compared with conventional bulk amplifier medium, the LCOF has an outstanding advantage, that is, because of lens coupling and its special waveguide structure the pump self-SBS presents a small spot with a small angular spread shown in Fig. 6(d) instead of a large diverging speckle. Therefore, this self-SBS noise is easily separated and removed.

When E_{pin} is chosen as 220 μJ , the SAF is then measured by decreasing E_{sin} , as Fig. 7(b) shows. The SAF of 1.3×10^6 for the input signal of $4 \times 10^{-12}\text{J}$ is achieved. It is apparent that the SAF of LCOF is lower than that of bulk liquid amplifier for the input signal with the same energy [19]. On one hand, this is attributed to the lower pump energy, since the smaller core diameter and hence smaller sectional area of the LCOF give rise to higher pump power density, to protect the LCOF and its coupling ends, the pump energy must be controlled below their damage threshold; On the other hand, larger incidence angle of the pump beam in this large core-diameter LCOF results in poorer overlap between the pump and signal beams. However, owing to higher Brillouin gain coefficient of the liquid medium, the LCOF SAF is much higher than the crystal fiber's [20].

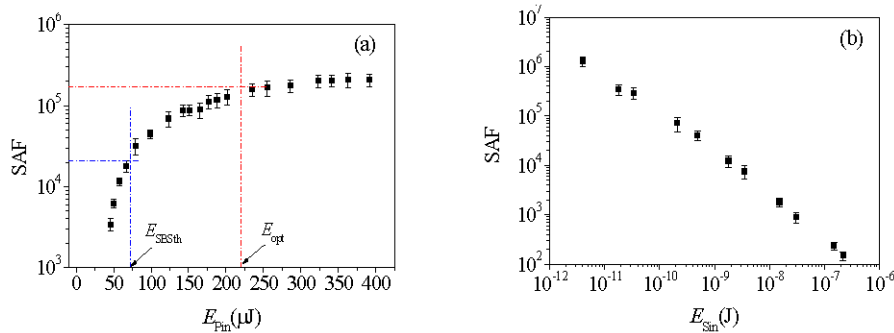


Fig. 7. SAF versus (a) E_{pin} and (b) E_{sin} .

5. Conclusion

We have demonstrated that a DHB can be generated and at the same time amplified through a LCOF contained CS_2 . The dependences of the DSS of the DHB on the incident angle of the laser beam are simulated by Zemax, and the principle of non-collinear Brillouin amplification of the DHB is also discussed. The relevant experimental verifications are performed. The results show that the DSS of DHB can be adjusted in a wide range by changing the incident angle of the laser, meanwhile, the DHB energy can be amplified with high gain based on non-collinear Brillouin amplification. For a weak DHB of 4pJ, an amplification of 1.3×10^6 is achieved. By optimizing the system configurations the quality and stability of the DHB is expected to be further improved. We believe the DHB that can be amplified flexibly should find broad application prospect.

Acknowledgments

This work is supported by the National Natural Science Foundation of China (Grant No. 61078004), the China Postdoctoral Science Foundation (Grant No. 20100481017), Technology of Education the Bureau of Heilongjiang Province, China (Grant No. 11521048) and Graduates' innovation fund of HUST (Grant No. 111021422).